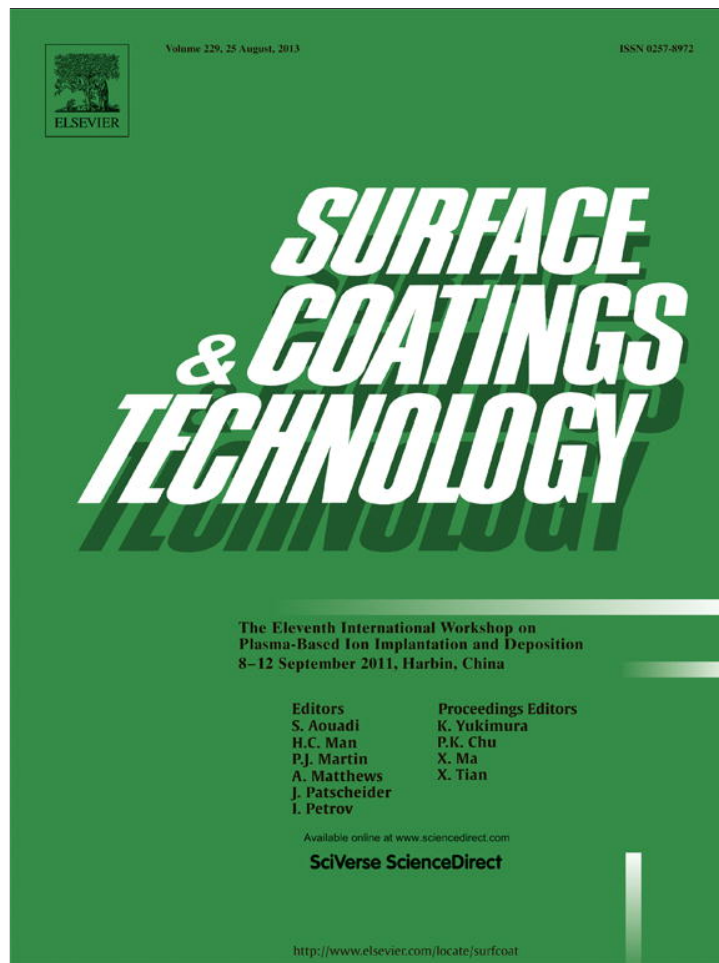


Provided for non-commercial research and education use.
Not for reproduction, distribution or commercial use.



This article appeared in a journal published by Elsevier. The attached copy is furnished to the author for internal non-commercial research and education use, including for instruction at the authors institution and sharing with colleagues.

Other uses, including reproduction and distribution, or selling or licensing copies, or posting to personal, institutional or third party websites are prohibited.

In most cases authors are permitted to post their version of the article (e.g. in Word or Tex form) to their personal website or institutional repository. Authors requiring further information regarding Elsevier's archiving and manuscript policies are encouraged to visit:

<http://www.elsevier.com/authorsrights>



Contents lists available at SciVerse ScienceDirect

Surface & Coatings Technology

journal homepage: www.elsevier.com/locate/surfcoat

The different N concentrations induced cytocompatibility and hemocompatibility of MWCNTs with CN_x coatings

M.L. Zhao^a, D.J. Li^{a,*}, M.X. Guo^a, Y.T. Zhang^a, H.Q. Gu^{b,c}, X.Y. Deng^a, R.X. Wan^{b,c}, X. Sun^d

^a College of Physics and Electronic Information Science, Tianjin Normal University, Tianjin 300387, China

^b Tianjin Institute of Urological Surgery, Tianjin Medical University, Tianjin 300070, China

^c Ninth People's Hospital, Shanghai Jiao Tong University, School of Medicine, Shanghai 200011, China

^d Department of Mechanical & Materials Engineering, University of Western Ontario, London, ON, Canada

ARTICLE INFO

Available online 16 September 2012

Keywords:

Multiwalled carbon nanotubes
CN_x
N/C atomic composition ratio
Cytocompatibility
Hemocompatibility

ABSTRACT

Carbon nitride coatings were deposited on the multiwalled carbon nanotubes (MWCNTs) which were prepared by chemical vapor deposition (CVD) using ion beam assisted deposition (IBAD) system. The morphology of the MWCNTs as well as variation in composition and chemical bonds between atoms in the coatings were measured using transmission electron microscopy (TEM) and X-ray photoelectron spectroscopy (XPS). The relationship between N/C atomic composition ratio and chemical bonding states and cytocompatibility and hemocompatibility of the MWCNTs with CN_x coatings was investigated using fibroblast cell (L929) adhesion and blood clotting assays. The results revealed that the higher N/C or sp²C–N/sp³C/N ratio stimulated the cell growth, proliferation, and spreading and prolonged the kinetic blood-clotting time and recalcification time.

© 2012 Elsevier B.V. All rights reserved.

1. Introduction

Since the discovery of carbon nanotubes (CNTs) in 1991 [1], a wide range of current and/or future applications of CNTs has been proposed owing to their amazing electronic, mechanical, and structural properties [2,3]. The advent of engineered CNTs in commercial and industrial applications raised concerns about the potential impacts of CNTs on human health and environmental safety [4–7]. The biological compatibility is determined mainly by the chemical composition of the implant material. Properties of the biomaterial surface, such as its energy, relief and roughness, are important for the hemocompatibility and the deposition of cells [8,9]. So, surface modification of CNTs will cause an important impact on its clinical applications.

In considering surface modification of biomaterials, carbon nitride (CN_x) appeared to have an advantage in that they show better biocompatibility. CN_x coating used to modify the properties of the CNTs surface may change the ratio of proteins absorbed on the surface and, hence, improve adhesion and growth of cells [9–12]. In this work, we married multiwalled carbon nanotubes (MWCNTs) with CN_x coatings to study the effects of N/C atomic composition ratio or sp³C and sp²C bonds on biocompatibility. Recently, there have been few studies on the biocompatibility of CN_x coating which deposited on the surface of the MWCNTs, especially for the mechanism of

biocompatibility from sp³C or sp²C bond. The aim of this work was to study the biocompatibility of the MWCNTs with CN_x coatings by investigating blood-clotting time and cell adhesion in cultures, and obtain the insight into the function of N/C atomic composition ratio or sp³C and sp²C bonds in the contact between the tissue and material surface.

2. Experimental details

2.1. Preparation and measurement of the MWCNTs with CN_x coatings

The synthesis of carbon film coated on a SiO₂ substrate was carried out using a chemical vapor deposition (CVD) system at 750 °C for half an hour. The gas flow rates of argon and ethylene were 250 sccm and 100 sccm respectively. The carbon film should be responsible for the adhesion strength enhancement between the SiO₂ substrate and MWCNTs. After that, the MWCNTs and SDS were dissolved in deionized water with ultrasonic dispersion for 5 min. After centrifugation of 10 min, the upper supernatant was directly sprayed onto the SiO₂ substrates coated with carbon film with air brush pistol at 100 °C to form MWCNTs. Then the MWCNTs were immersed into deionized water for 10 min and then dried in a dry oven at 80 °C for 30 min to remove the SDS [13,14]. CN_x coatings were deposited on the surfaces of the MWCNTs by ion beam assisted deposition (IBAD) system, as shown in Fig. 1. In this process, the chamber was evacuated to a base pressure lower than 3.0 × 10^{−4} Pa prior to the deposition. Graphite target (70 × 70 mm²) was sputtered by Ar⁺ from Kaufman

* Corresponding author. Tel./fax: +86 22 23766519.
E-mail address: dejunli@mail.tjnu.edu.cn (D.J. Li).

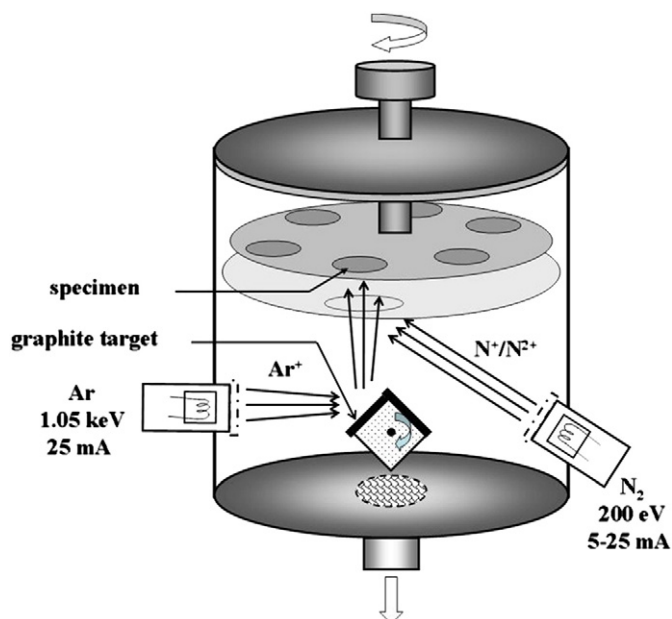


Fig. 1. The schematic of IBAD.

gun at 1.05 keV/25 mA to deposit C coating at 2.0×10^{-2} Pa, and the resulting coating was simultaneously bombarded at a N^{n+} beam current of 200 eV/5–25 mA from Kaufman gun to prepare CN_x coatings with different N/C atomic composition ratios on the MWCNTs for 30 min. The current densities of N^{n+} are 0.25–1.27 mA/cm².

X-ray photoelectron spectroscopy (XPS) was performed to investigate N/C atomic composition ratio and chemical bonding states of the surfaces using a PHI5000 versa probe system (Al ($K\alpha$) X-ray source 1486.6 eV). The detailed morphologies of the MWCNTs before and after CN_x coating were characterized using a JOEL JEM2100 high-resolution transmission electron microscope (HRTEM) and a field-emission scanning electron microscope (FESEM, Hitachi S-3000N). A CAM KSV021733 optical contact-angle inclinometer (Nunc, Finland) was also used to measure the contact angle of the samples.

2.2. Cell-adhesion and blood-clotting assays

Mouse fibroblast cells (L929) were used to investigate the cytocompatibilities of the four MWCNTs with CN_x coatings. L929 cells were cultured in Earle's salt supplemented with 10% fetal bovine serum,

100 units/ml penicillin and 100 μ g/ml streptomycin. Cells were plated onto 75 mm² culture flasks and maintained at 37 °C in a humidified atmosphere with 5% CO₂ in air. They were released from culture flasks using a trypsin and phosphate buffer solution pH 7.4 (PBS). The inoculum density of the fibroblast cells is 2.5×10^4 cells/ml. After 1 to 7 days in the incubator (culture intervals of 0.5, 1, 2, 3, 5, and 7 days), the medium was removed and the cell monolayer was washed several times with PBS and then isolated by trypsin for enumeration. Confocal scanning laser microscopy (CSLM) (Nikon eclipse 90) and SEM were employed to observe cell morphology and stretching on the four samples.

Kinetic blood-clotting times were measured by the kinetic method. In this method, 0.1 ml of blood from a healthy adult rabbit was immediately dropped onto the surfaces of the samples. After a predetermined time, the samples were transferred into a beaker containing 50 ml of distilled water. The red blood cells which had not been trapped in a thrombus were hemolyzed, and the free hemoglobin was dispersed in the solution. The concentration of free hemoglobin in the solution was colorimetrically measured at 540 nm with a spectrophotometer. The optical density at 540 nm ($O.D._{540\text{ nm}}$) of the solution vs. time was plotted. In general, the $O.D._{540\text{ nm}}$ value decreases with blood clotting.

The recalcification times of the materials were measured by recording the interval time from introducing 0.1 ml of CaCl₂ solution into a test-tube containing the samples and 0.1 ml of rabbit plasma to finding white particles in the plasma.

3. Results and discussion

Fig. 2 shows SEM images of the MWCNTs, MWCNTs with $CN_{0.21}$ coatings (N^{n+} beam current of 25 mA) and MWCNTs with $CN_{0.27}$ coatings (N^{n+} beam current of 10 mA), respectively. The surface of the MWCNTs which has porous structure is rough, as shown in Fig. 2(a). And the water contact angle measured on the pristine MWCNTs is 124.86°. Generally speaking, a surface with water contact angle larger than 65° is defined as hydrophobic. So, the MWCNT without CN_x coating reveals hydrophobicity. Apparent thin film covering the MWCNTs can be observed after coated CN_x coating on them (Fig. 2(b, c)). Samples' surfaces are flatter and there are few voids as shown in Fig. 2(b, c). The contact angles of the MWCNTs with CN_x coatings drop to 37.63° and 47.01°, indicating hydrophilic surfaces due to CN_x coatings.

To investigate detail morphologies of the MWCNTs with CN_x coating, HRTEM characterizations are performed, as shown in Fig. 3. The tubular structures of these two samples are seen in these figures. MWCNTs' outer diameters are approximately 30–50 nm, and the wall thicknesses are approximately 10 nm, as shown in Fig. 3(a, b). It can be seen that the graphite layers of the MWCNTs are generally parallel to each other with small curvature. Before depositing the CN_x coating on the MWCNTs, the deposition rates of the CN_x films

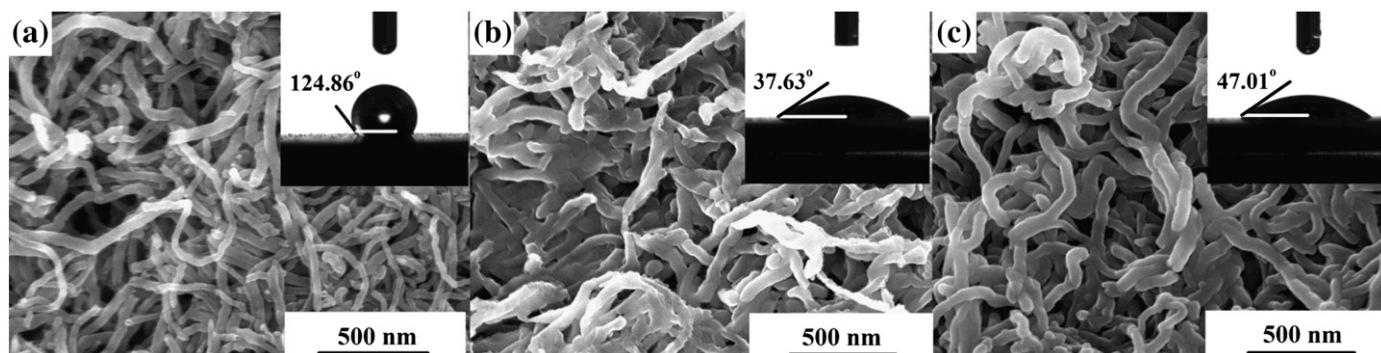


Fig. 2. SEM images of the MWCNTs (a), MWCNTs with $CN_{0.21}$ coating (b) and MWCNTs with $CN_{0.27}$ coating (c). The insets were their contact angle images, respectively.

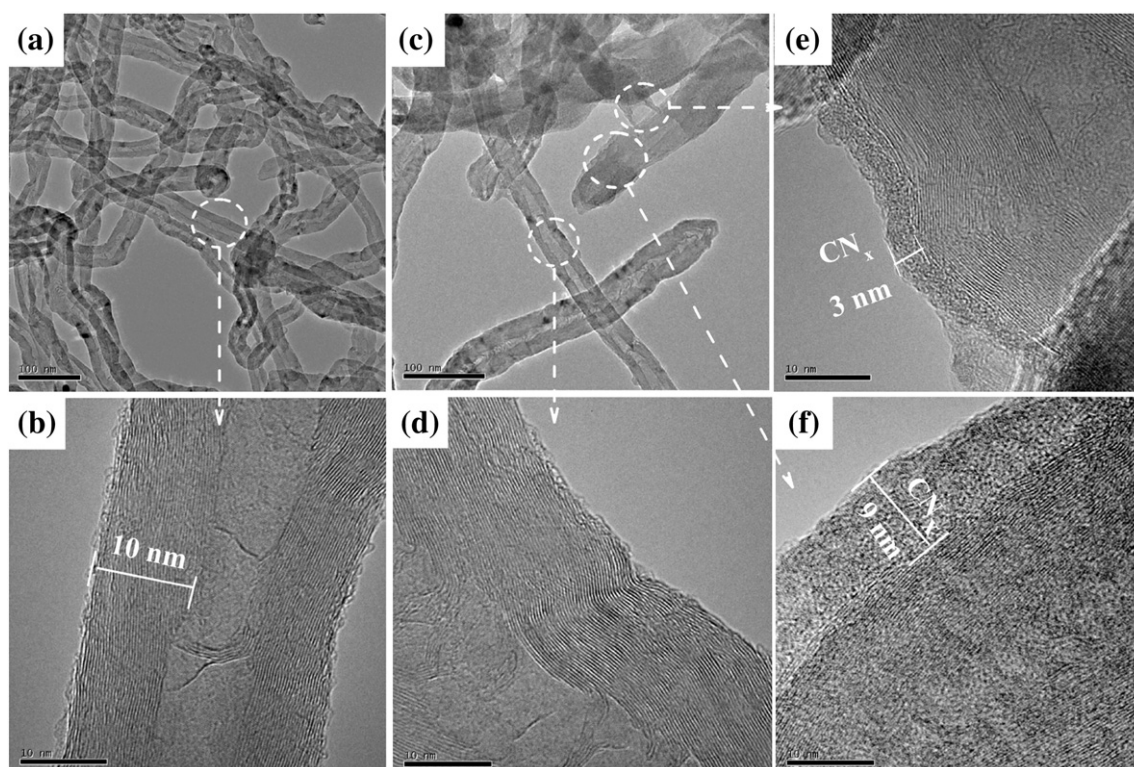


Fig. 3. HRTEM images of the MWCNTs without CN_x coating (a,b) and with $CN_{0.21}$ coating (c–f) at different magnification times.

on the Si(100) substrates with variation of Nitrogen beam current have been examined. The film thicknesses for the samples prepared with variation of Nitrogen ion beam are all 15 nm, which means that deposition rates were 0.5 nm/min. Fig. 3(c–f) shows HRTEM images of the MWCNTs with $CN_{0.21}$ coating at different magnification times. The structures of the CN_x coated on the MWCNTs are clear (shown by white rulers). Because the CN_x coatings were deposited by the IBA method on the MWCNTs layered on the substrates, it results in selective deposition on the top surface of the MWCNTs. The underside of the MWCNTs in the top layer and the other MWCNTs underneath cannot be coated in the same way, as shown in Fig. 3(d). And for some of the MWCNTs with CN_x coating on top, the CN_x layer is thick (Fig. 3(f)), for others beneath it's thinner (Fig. 3(e)). Because the cells only adhere to the top surface of the MWCNTs with CN_x coating when they were seeded on the samples, the underside of the MWCNTs in the top layer and the other MWCNTs underneath which cannot be coated with CN_x do very little affecting the results of the experiment.

XPS is used to characterize the differences in surface chemical bonding states and nitrogen concentration of the MWCNTs with CN_x coatings deposited by different N^{n+} beam current densities, which would cause obvious changes in the hemocompatibility and the cell adhesion. The chemical bonding states are obtained by subtracting the background with the Shirley's method and deconvoluting the spectra by a curve-fitting method using a non-linear least squares fitting to a mixed Gaussian–Lorentzian product function. From the XPS analysis, the N concentration of four MWCNTs with CN_x coatings is shown in Table 1. The N/C atomic composition ratios are 0.21, 0.27, 0.26, 0.21 corresponding to the N^{n+} beam currents of 5, 10, 15, 25 mA. We mark these samples successively by CN-1, CN-2, CN-3, CN-4 and divide them into two groups according to the similar N/C ratio.

Fig. 4 shows the high-resolution XPS core-level spectra of C_{1s} and N_{1s} of the four samples. Tables 2 and 3 indicate their C_{1s} and N_{1s} peak positions and areas. The C_{1s} peak is decomposed into five Gaussian

components, referring to the bonds: sp^2C-C (~284.7 eV), sp^3C-C (~285.6 eV), sp^2C-N (~286.4 eV), sp^3C-N (~287.9 eV), and sp^2C-O (~288.6 eV) [15–18]. The N_{1s} peak has also revealed sp^2 and sp^3C-N bonds at 400.1 and 398.7 eV respectively [17,18]. From the data, it is indicated clearly that with the beam current increasing, the ratio of the tetrahedral sp^3C-C bonds decreases and the ratio of the sp^2C-C bonds increases, while the diamond-like sp^3C-N and sp^2C-N bonds have the opposite changes. This difference reveals a strong change in the surface chemical bonding states.

The relationship between the sp^2C/sp^3C and the cell adhesion is shown in Fig. 5. For group 1, the cell adhesion numbers on CN-1 are more than CN-4 from days 1 to 7, despite that the cell numbers reduce gradually after 5 days. In addition, the cell concentrations on CN-2 are larger than CN-3, which sustains an increase throughout the incubation period. As shown in SEM images of CN-1 and CN-3, the adhered cells spread flat with rich pseudopod which suggests that the MWCNTs with CN_x coating provide better conditions for the cellular spreading and the pseudopod spreading. Maximum numbers of L929 cells adhered to CN-1, CN-2 and CN-3 are almost the same. The cell adhesion numbers also increase with the sp^2C-N/sp^3C-N and sp^3C-C/sp^2C-C increasing in the same N/C ratio. These results indicate that the major factor causing cell adhesion is not only higher nitrogen content, but also the higher sp^2C-N/sp^3C-N or sp^3C-C/sp^2C-C ratio.

Table 1
The atom content percent (%) and N/C ratio of the MWCNTs with CN_x coatings.

Samples	CN-1	CN-2	CN-3	CN-4
Beam current (mA)	5	10	15	25
N (%)	17.63	21.34	20.93	17.54
N/C (atm)	0.21	0.27	0.26	0.21

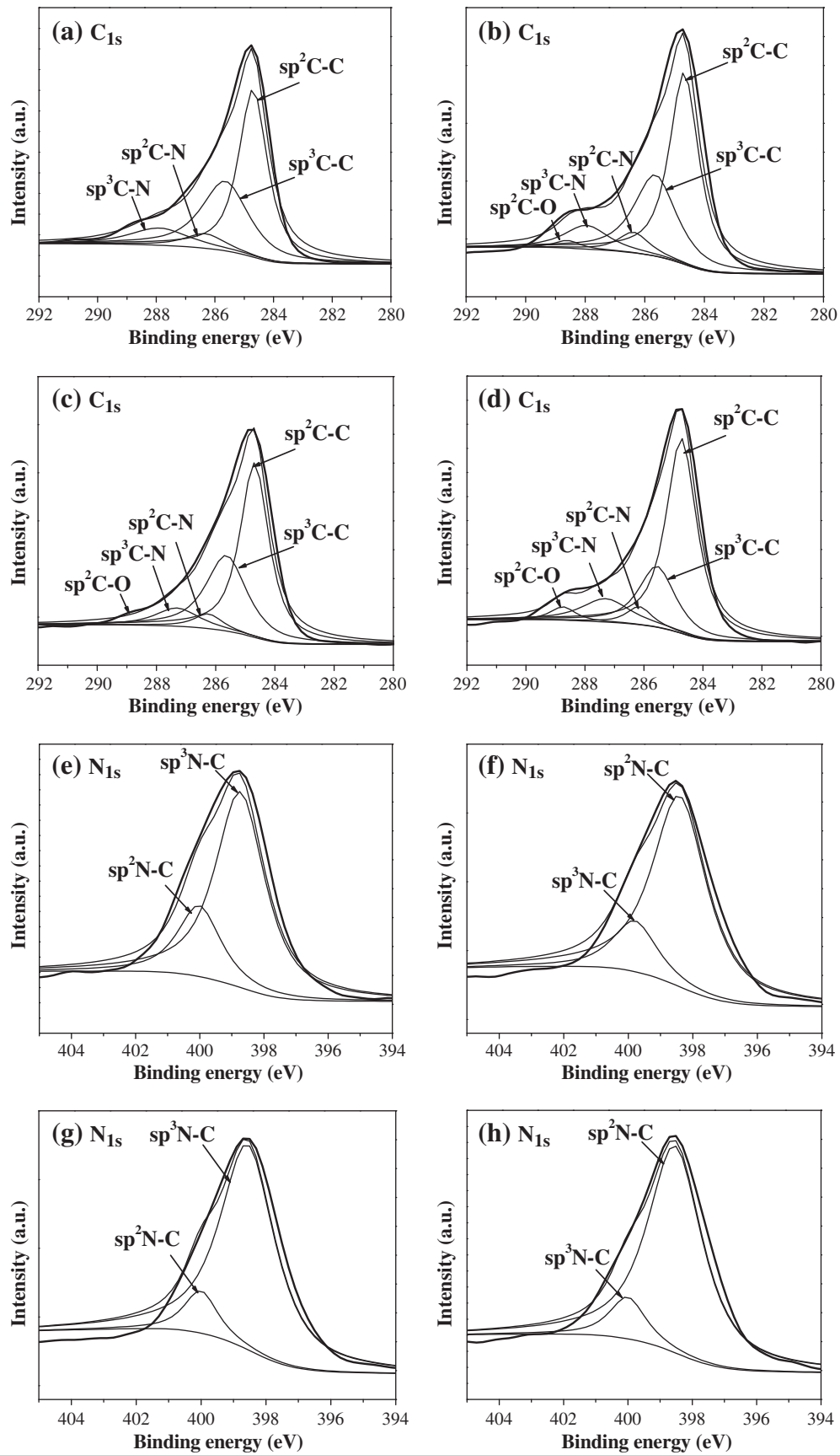


Fig. 4. C_{1s} XPS spectra of CN-1 (a), CN-2 (b), CN-3 (c), CN-4 (d), and N_{1s} XPS spectra of CN-1 (e), CN-2 (f), CN-3 (g), CN-4 (h).

Table 2
C_{1s} peaks of the MWCNTs with CN_x coatings.

Samples	Peak position (eV)				Peak area ratio			
	CN-1	CN-2	CN-3	CN-4	CN-1	CN-2	CN-3	CN-4
sp ² C–C	284.7	284.7	284.7	284.7	0.597	0.699	0.714	0.780
sp ³ C–C	285.6	285.6	285.6	285.6	0.403	0.301	0.286	0.220

Table 3
N_{1s} peaks of the MWCNTs with CN_x coatings.

Samples	Peak position (eV)				Peak area ratio			
	CN-1	CN-2	CN-3	CN-4	CN-1	CN-2	CN-3	CN-4
sp ² C–N	398.7	398.4	398.6	398.5	0.761	0.822	0.889	0.884
sp ² C–N	400.0	399.8	400.0	400.0	0.239	0.178	0.111	0.116

In addition, using immunofluorescence techniques, microfilaments and microtubules are stained, which are the main components of the cytoskeleton. Meanwhile the nuclear DNA stains with a different fluorescent dye and then combines the three photographs taken by confocal scanning laser microscopy (CSLM) in the same viewing field, with same exposure times, as shown in Fig. 6. The CSLM images show the morphology of mouse-fibroblast cells fixed on the surface of four samples after the incubation of one day. It can be seen from Fig. 6 that typical triangular cells adhere to the surface of all the samples. With the sp²C–N/sp³C–N and sp³C–C/sp²C–C increasing, the cell numbers on the materials in the same N/C ratio are larger. Cells spread more flat and there were more pseudopodia and microvilli on the cell surface. Fig. 6 also suggests that the samples with higher N/C ratio provide better

conditions for the fibroblast growth, because the cell numbers on CN-2 and CN-4 are larger than the two other samples.

From these results, we consider the mechanism for improving cell adhesion. Protein absorption is an early in vivo event in the interaction between implanted biomaterial and living tissue. All proteins have NH₂ and COOH groups at the ends, where, according to Takashima et al. [19], the NH tends to be positively charged and the COOH negatively charged. Thus, a surface with an organized arrangement of functional groups can act as a site for the cell growth [20]. The MWCNTs with CN_x coatings include sp²C–N and sp³C–N bonds at the surface and polarize at the surface due to the difference in electronegativity between carbon and nitrogen [21]. So the higher N/C ratio means more sites for the cell growth, which explains why CN-2 and CN-3 have more cells on their surfaces. With sp²C–N/sp³C–N ratio increasing, there are more unsaturated bonds in the samples, which causes the cell adhesion numbers to increase with the number of protein attached the material surface. Thus, the cell adhesion numbers increase with the sp²C–N/sp³C–N increasing in the same N/C ratio. For group 1, the cell adhesion numbers on CN-1 are more than CN-4. And the cell concentrations on CN-2 are larger than CN-3 throughout the incubation period for group 2.

Thrombus formation occurs when a biomaterial surface comes into contact with blood, prompted by rapid adsorption of plasma proteins onto the surface within the first few seconds of contact. This adsorption is regarded as the first major event in the coagulation process [22]. Among the plasma proteins, fibrinogen is regarded as the key protein that triggers platelet adhesion, activation and aggregation. Subsequently, coagulation factors are released, initiating the coagulation cascade and the eventual formation of a thrombus [23]. The kinetic blood-clotting time of all the samples is shown in Fig. 7. The higher optical density of the hemolyzed hemoglobin solution which changes with time means the better thromboresistance. The time when the optical density is 0.1 is defined as the kinetic blood-clotting time [17]. The result shows that the blood-clotting times of CN-3 (50 min) and CN-4 (41 min) are longer

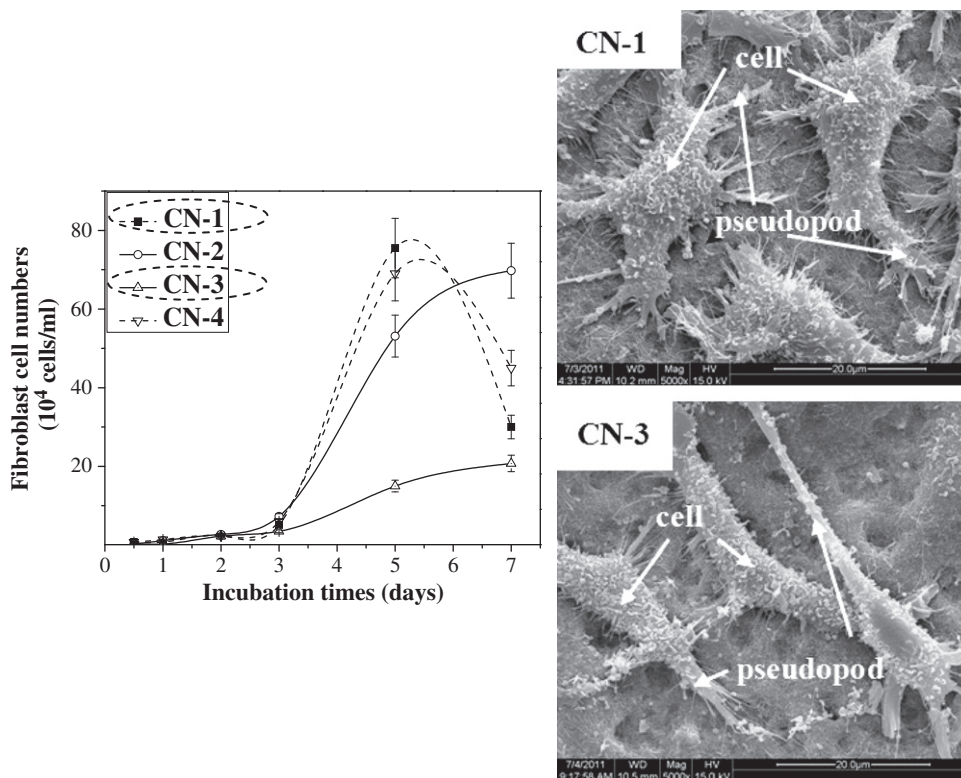


Fig. 5. L929 mouse fibroblast cell numbers on the MWCNTs with CN_x coatings vs. incubation time. The insets are their SEM images.

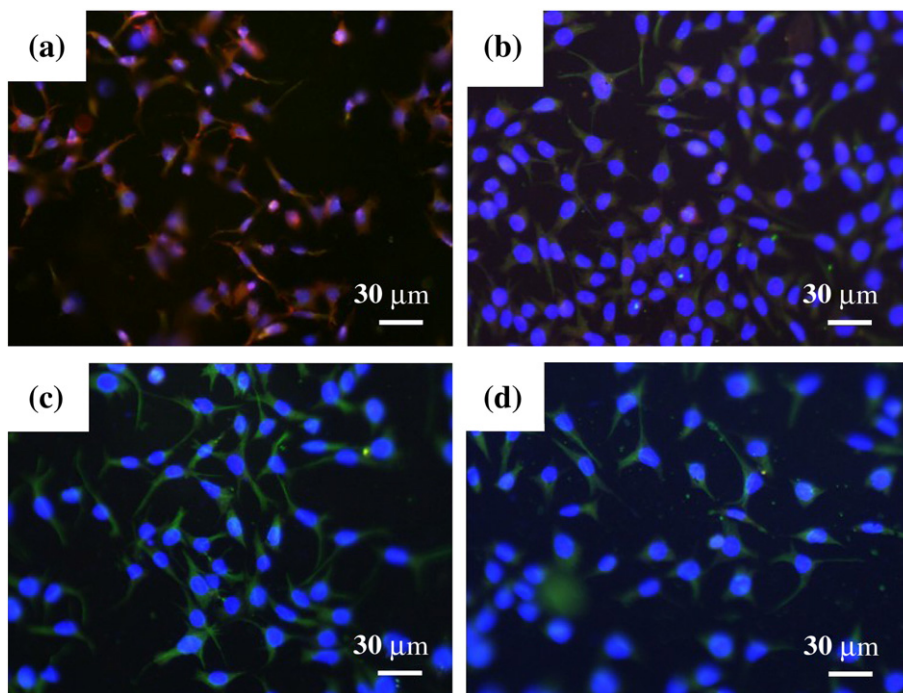


Fig. 6. CSLM images of mouse fibroblast cells fixed on CN-1 (a), CN-2 (b), CN-3(c), CN-4 (d).

than CN-2 (31 min) and CN-1 (40 min) respectively, which means the better thromboresistance of CN-3 and CN-4.

Recalcification time is also obtained using venous blood of rabbit. The longer recalcification time of the materials suggested the better anti-coagulability. Fig. 8 shows the recalcification time of the four samples. The same results among CN-1, CN-2, CN-3 and CN-4 can be observed. Their change tendency implies that higher sp^2C-N/sp^3C-N ratios in the same N/C ratio can prolong recalcification time.

Factors influencing the hemocompatibility of biomaterials lie in several aspects: surface roughness, hydrophilicity or hydrophobicity, surface charge density and so on [24]. Many studies have demonstrated that higher hydrophilicity and superficial energy appeared to be the primary factor improving the surface blood-contacting properties [25,26]. Materials with high hydrophilicity and surface energy are likely to be covered by a protein-dominating 'conditioning film'

that may yield good hemocompatibility [27,28]. As shown in Fig. 9, the contact angles of CN-1, CN-2, CN-3 and CN-4 are about 40.08° , 47.01° , 30.77° and 37.63° , respectively. This explains why CN-3 and CN-4 exhibit better thromboresistance.

In addition, the hemoglobin, platelet and a few of plasma protein in blood tend to be negatively charged. Usually the material surface with more unsaturated bonds in electronegativity has better thromboresistance according to principle of same electric charge mutual repulsion. However, many factors, such as protein adsorption on the material surface and positive charge in blood are all assumed to result in positive effects on the hemocompatibility of the materials. Thus, the suitable density of charge will promote the hemocompatibility [29]. A suitable ratio of sp^3C-N to sp^2C-N can provide the optimum density of charge to promote the hemocompatibility, which is the possible reason for better thromboresistance for the CN-3 and CN-4 samples.

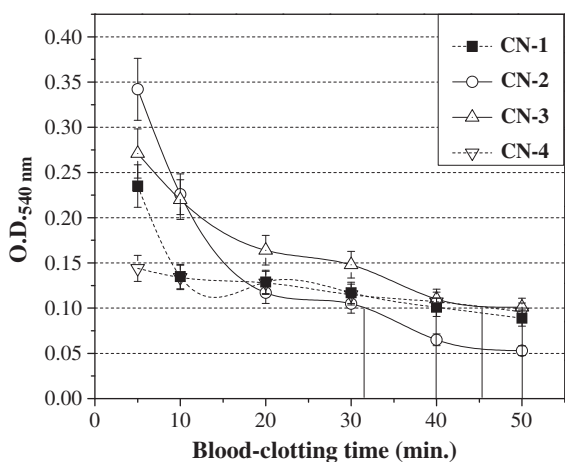


Fig. 7. The $O.D._{540\text{ nm}}$ values of the MWCNTs with CN_x coatings vs. blood-clotting time.

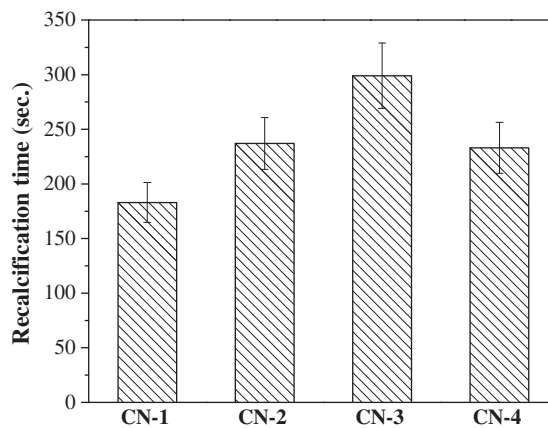


Fig. 8. Recalcification times of the MWCNTs with CN-1, CN-2, CN-3, and CN-4.

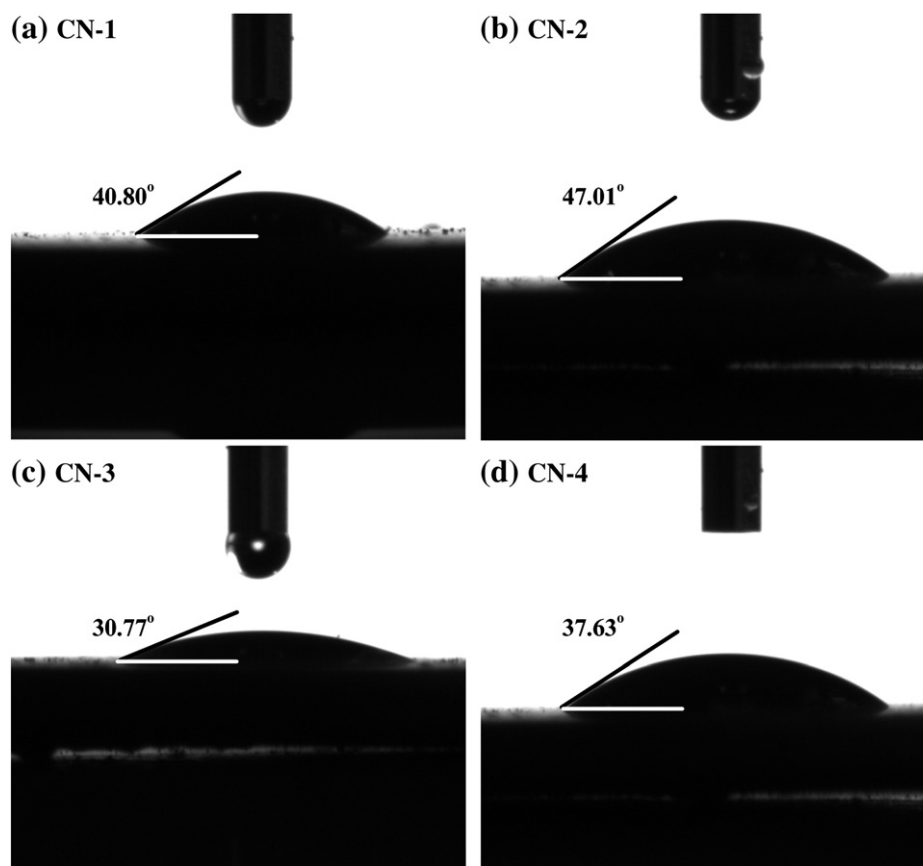


Fig. 9. The contact angle images of CN-1 (a), CN-2 (b), CN-3 (c), and CN-4 (d).

4. Conclusions

In this work, we deposited about 15 nm-thick CN_x coatings with different N/C atomic composition ratios on the MWCNTs. From the XPS analyses we found that the high N/C atomic composition ratio can increase the contents of the sp^2C-C bonds and the unsaturated degree of the N-groups of the coatings. The comparison of the cytocompatibility and hemocompatibility between the MWCNTs with different N/C ratio CN_x coatings displayed that the high N/C and sp^2C-N/sp^3C-N ratios might accelerate L929 cell adhesion and proliferation, while shortened the kinetic blood-clotting time and recalcification time. The mechanism of N/C and sp^2C-N/sp^3C-N ratios affecting biocompatibility is very complicated. Long-term effects need to be studied with further in vivo assays.

Acknowledgments

This work was supported by National Natural Science Foundation of China (11075116, 51272176), National Basic Research Program of China (973 Program, 2012CB933604), the Open Research Fund of the State Key Laboratory of Bioelectronics, Southeast University, and the Key Laboratory of Beam Technology and Material Modification of the Ministry of Education, Beijing Normal University, China.

References

- [1] S. Iijima, Nature 354 (1991) 56.
- [2] A. Jorio, G. Dresselhaus, M.S. Dresselhaus, in: Carbon Nanotubes, Advanced Topics in the Synthesis, Structure, Properties and Applications, Springer, Berlin, 2008, p. 1.
- [3] F.S. Lu, L.R. Gu, M.J. Mezziani, X. Wang, P.G. Luo, L.M. Veca, L. Cao, Y.P. Sun, Adv. Mater. 21 (2009) 139.
- [4] K.M. Kulinowski, V.L. Colvin, ACS Symp. Ser. 890 (2005) 21.
- [5] P. Christian, F. Von der Kammer, M. Baalousha, T. Media Hofmann, Ecotoxicology 17 (2008) 326.
- [6] S.J. Klaine, P.J.J. Alvarez, G.E. Batley, T.F. Fernandes, R.D. Handy, D.Y. Lyon, S. Mahendra, M.J. McLaughlin, J.R. Lead, Environ. Toxicol. Chem. 27 (2008) 1825.
- [7] M.F. Hochella, S.K. Lower, P.A. Maurice, R.L. Penn, N. Sahai, D.L. Sparks, B.S. Twining, Science 319 (2008) 1631.
- [8] T.M. Lee, E. Chang, C.Y. Yang, Biomaterials 25 (2004) 23.
- [9] D.B. Barbara, W.H. Thomas, D.D. David, Z. Schwartz, Biomaterials 17 (1996) 137.
- [10] R. Hauert, Diamond Relat. Mater. 12 (2003) 583.
- [11] E.B. Makarova, I.Sh. Trakhtenberg, A.B. Osipenko, V.A. Muhachev, in: Proceedings of the First Congress of the Orthopedic Traumatologists of Ural Federal Region "High Technologies in Traumatology and Orthopedics: Organization, Diagnostics, Treatment, Rehabilitation, Formation", Russia, 2005, p. 348.
- [12] E.M. Eropkina, E.G. Mamaeva, M.Yu. Eropkin, V.M. Mashkov, in: Vestnik of Traumatology and Orthopedics of N.N.Priorova, Russia, 2004, p. 18.
- [13] X. Yu, R. Rajamani, K.A. Stelson, T. Cui, Sensors Actuators 132 (2006) 626.
- [14] L. Xiao, Nano Lett. 8 (2008) 4539.
- [15] T. Shirasaki, F. Moguet, L. Lozano, A. Tressaud, G. Nansé, E. Papire, Carbon 37 (1999) 1891.
- [16] G. Nansé, E. Papirer, P. Fioux, F. Moguet, A. Tressaud, Carbon 35 (1997) 515.
- [17] M. Tabbal, P. Merei, S. Moisa, M. Chaker, A. Recard, M. Moisan, Appl. Phys. Lett. 69 (1996) 1698–1700.
- [18] P. Xu, J.J. Li, Q. Wang, Z.L. Wang, C.Z. Gu, Z. Cui, J. Appl. Phys. 101 (2007) 14312.
- [19] S. Takemoto, Y. Kusudo, K. Tsuru, S. Hayakawa, A. Osaka, S. Takashima, J. Biomed. Mater. Res. 69A (2004) 544.
- [20] Z.R. Wu, M. Zhang, F.Z. Cui, Surf. Coat. Technol. 201 (2007) 5710.
- [21] T. Yokota, T. Terai, T. Kobayashi, M. Iwaki, Nucl. Inst. Methods Phys. Res. B 242 (2006) 48.
- [22] L.B. Koh, I. Rodriguez, S.S. Venkatraman, Acta Biomater. 5 (2009) 3411.
- [23] L. Feng, J.D. Andrade, Washington, DC: American Chemical Society, 1995, pp. 66–79.
- [24] B.A. Weisenberg, D.L. Mooradian, J. Biomed. Mater. Res. 60 (2002) 283.
- [25] P.J. Dynes, J. Adhes. 6 (1974) 195.
- [26] J.S. Laura, L.W. Jennifer, G.M. Antonios, Biomaterials 20 (1999) 683.
- [27] B. Ivarsson, I. Lundstrom, CRC Crit. Rev. Biocomput. 2 (1986) 1.
- [28] R.E. Baier, J. Biomech. Eng. 104 (1982) 257.
- [29] L. Zhang, M. Chen, Z.Y. Li, D.H. Chen, S.R. Pan, Mater. Lett. 62 (2008) 1040.